

Opening Up the Neural Network Classifier for Shap Score Computation

Leopoldo Bertossi¹ and Jorge E. León²

¹SKEMA Business School, Montreal, Canada

² Universidad Adolfo Ibáñez (UAI), Santiago, Chile

leopoldo.bertossi@skema.edu, jorgleon@alumnos.uai.cl

Abstract

We address the problem of efficiently computing Shap explanation scores for classifications with machine learning models. With this goal, we show the transformation of binary neural networks (BNNs) for classification into deterministic and decomposable Boolean circuits, for which knowledge compilation techniques are used. The resulting circuit is treated as an open-box model, to compute Shap scores by means of a recent efficient algorithm for this class of circuits. Detailed experiments show a considerable gain in performance in comparison with computing Shap directly on the BNN treated as a black-box model.

1 Introduction

In recent years, in which more sophisticated machine learning (ML) models have emerged, and their uses have become widespread, there has been a growing demand for methods to explain and interpret the results they produce. For example, explanations for why a loan application is rejected, or why a medication is recommended, or why a candidate is selected for a job, etc. In this work, we concentrate on explanations for binary classification models that assign one of two labels to the inputs, say 0 or 1.

Explanations come in different forms, and can be obtained through different approaches. A common one assigns *attribution scores* to the features values associated to an input that goes through an ML-based model, to *quantify* their relevance for the obtained outcome. We concentrate on *local* scores, i.e. associated to a particular input, as opposed to a global score that indicated the overall relevance of a feature.

A popular local score is **Shap** (Lundberg and Lee 2017), which is based on the Shapley value that has introduced and used in coalition game theory and practice for a long time (Shapley 1953; Roth 1988). Another attribution score that has been recently investigated in (Bertossi et al. 2020; Bertossi 2022) is **Resp**, the responsibility score (Chockler and Halpern 2004) associated to *actual causality* (Halpern and Pearl 2005). In this work we concentrate on the **Shap** score, but the issues investigated here would be also interesting for other scores.

Shap scores can be computed with a black-box or an open-box model (Rudin 2019). With the former, we do not know or use its internal components, but only its input/output relation. This is the most common approach. In

the latter case, we can have access to its internal structure and components, and we can use them for score computation. It is common to consider neural-network-based models as black-box models, because their internal gates and structure may be difficult to understand or process when it comes to explaining classification outputs. However, a decision-tree model, due to its much simpler structure and use, is considered to be open-box for the same purpose.

Even for binary classification models, the complexity of Shap computation is provably hard, actually $\#P$ -hard for several kinds of binary classification models, independently from whether the internal components of the model are used when computing Shap (Bertossi et al. 2020; Arenas et al. 2021a; Arenas et al. 2021b). However, there are classes of classifiers for which, using the model components and structure, the complexity of Shap computation can be brought down to polynomial time (Lundberg et al. 2020; Arenas et al. 2021b; Van den Broeck et al. 2021).

A polynomial time algorithm for Shap computation with *deterministic and decomposable Boolean circuits* (dDBCs) was presented in (Arenas et al. 2021b). From this result, the tractability of Shap computation can be obtained for a variety of Boolean circuit-based classifiers and classifiers that can be represented as (or compiled into) them. In particular, this holds for *Ordered Binary Decision Diagrams* (OBDDs) (Bryant 1986), decision trees, binary neural networks (BNNs), and other established classification models that can be compiled into OBDDs (Shi et al. 2020; Darwiche and Hirth 2020; Narodytska et al. 2018). Similar results can be obtained for *Sentential Decision Diagrams* (SDDs) (Darwiche 2011b), which can be seen as dDBCs, and form a convenient *knowledge compilation* target language (Darwiche and Marquis 2002; Van den Broeck and Darwiche 2015). In (Van den Broeck et al. 2021), through a different approach, tractability of Shap computation was obtained for a collection of classifiers that intersect with that in (Arenas et al. 2021b).

In this work, we concentrate on explicitly developing this approach to the efficient computation of Shap for *binary neural networks* (BNNs). For this, and inspired by (Shi et al. 2020), a BNN is transformed into a dDBC using techniques from *knowledge compilation* (Darwiche and Marquis 2002), an area that investigates the transformation of (usually) propositional theories into an equivalent one with a

canonical syntactic form that has some good computational properties, e.g. tractable model counting. The compilation may incur in a relatively high computational cost (Darwiche and Marquis 2002; Darwiche 2011a), but it may still be worth the effort when a particular property will be checked often, as is the case of explanations for the same BNN.

More specifically, we describe in detail how a BNN is first compiled into a propositional formula in Conjunctive Normal Form (CNF), which, in its turn, is compiled into an SDD, which is finally compiled into a dDBC. We show how **Shap** is computed on the resulting circuit via the efficient algorithm in (Arenas et al. 2021b). This compilation is performed once, and is independent from any input to the classifier. The final circuit can be used to compute **Shap** scores for different input entities.

We also make experimental comparisons between this open-box and circuit-based **Shap** computation and that based directly on the BNN treated as a black-box, i.e. using only its input/output relation. We perform comparisons in terms of computation time and alignment of **Shap** scores.

For our experiments, we consider real state as an application domain, where house prices depend on certain features, which we appropriately binarize.¹ The problem consists in classifying property blocks, represented as entity records of thirteen feature values, as *high-value* or *low-value*. This is a binary classification problem for which a BNN is first learnt, and then used.

To the best of our knowledge, our work is the first at using knowledge compilation techniques for efficiently computing **Shap** scores, and the first at reporting experiments with the polynomial time algorithms for **Shap** computation on binary circuits. We confirm that **Shap** computation via the dDBC vastly outperforms the direct **Shap** computation on the BNN. It is also the case that the scores obtained are fully aligned, as expected since the dDBC represents the BNN.

Compilation of binary classifiers, in particular BNNs, into OBDDs was used in (Darwiche and Hirth 2020) to provide different kinds of explanations for outcomes, but not for **Shap** computation or any other kind of attribution score. In this work we concentrate only on explanations based on **Shap** scores. There are several other explanations mechanisms for ML-based classification and decision systems in general, and also specific for neural networks. C.f. (Guidotti et al. 2018) and (Ras et al. 2022) for surveys.

This paper is structured as follows. Section 2 contains background on **Shap** and Boolean circuits. Section 3 show in detail, by means of a running example, the kind of compilation of BNNs into dDBC we use for the experiments. Section 4 presents the experimental setup, and the results of our experiments with **Shap** computation. In Section 5 we draw some conclusions. Appendices A and B provide additional technical details for Section 3.

¹We use the California Housing Prices dataset available at <https://www.kaggle.com/datasets/camnugent/california-housing-prices>.

2 Preliminaries

In coalition game theory and its applications, the Shapley value is a established measure of the contribution by players to a shared wealth that is modelled as a game function. Given a set of players S , and a game function $G : \mathcal{P}(S) \rightarrow \mathbb{R}$, i.e. mapping subsets of players to real numbers, the general form of the Shapley value for a player $p \in S$ is:

$$\text{Shapley}(S, G, p) := \sum_{s \subseteq S \setminus \{p\}} \frac{|s|!(|S| - |s| - 1)!}{|S|!} (G(s \cup \{p\}) - G(s)). \quad (1)$$

It quantifies the contribution of p to G . It emerges as the only measure that enjoys certain desired properties (Roth 1988). Here all possible permutations of subsets of S , and of their complements, are considered. So, this value is the average of differences between having p or not in a subteam. To apply the Shapley value, one defines a game function G .

Now, consider a fixed entity $\mathbf{e} = \langle F_1(\mathbf{e}), \dots, F_N(\mathbf{e}) \rangle$ subject to classification. It has values $F_i(\mathbf{e})$ for features $\mathcal{F} = \{F_1, \dots, F_N\}$. These values are 0 or 1 for binary features, which is our case. In (Lundberg and Lee 2017; Lundberg et al. 2020), the Shapley value in (1) is applied with $\{F_1(\mathbf{e}), \dots, F_N(\mathbf{e})\}$ as the set of players, and the game function $\mathcal{G}_{\mathbf{e}}(s) := \mathbb{E}(L(\mathbf{e}') \mid \mathbf{e}'_s = \mathbf{e}_s)$, giving rise to the **Shap** score. Here, \mathbf{e}_s is the projection (or restriction) of \mathbf{e} on (to) the subset s of features, L is the label function associated to the classifier; 0 or 1 in our case. The \mathbf{e}' inside the expected value is an entity whose values coincides with those of \mathbf{e} for the features in s . Accordingly, for feature $F \in \mathcal{F}$, and entity \mathbf{e} , **Shap** becomes:

$$\text{Shap}(\mathcal{F}, \mathcal{G}_{\mathbf{e}}, F) = \sum_{s \subseteq \mathcal{F} \setminus \{F\}} \frac{|s|!(|\mathcal{F}| - |s| - 1)!}{|\mathcal{F}|!} [\quad (2) \\ \mathbb{E}(L(\mathbf{e}') \mid \mathbf{e}'_{S \cup \{F\}} = \mathbf{e}_{S \cup \{F\}}) - \mathbb{E}(L(\mathbf{e}') \mid \mathbf{e}'_s = \mathbf{e}_s)].$$

The expected value is defined on the basis of an underlying probability distribution on the entity population. **Shap** quantifies the contribution of feature value $F(\mathbf{e})$ to the outcome label.

In order to compute **Shap**, we only need function L , and none of the internal components of the classifier. Given that all possible subsets of features appear in its definition, **Shap** is bound to be hard to compute. Actually, for some classifiers, its computation may become $\#P$ -hard (c.f. (Arenas et al. 2021b) for some cases). However, in (Arenas et al. 2021b), it is shown that **Shap** can be computed in polynomial time for every *deterministic and decomposable Boolean circuit* (dDBC) used as a classifier. The circuit's internal structure is used in the computation (c.f. Section 4).

Figure 1 shows a Boolean circuit that can be used as a binary classifier, with input features x_1, x_2, x_3 . Their binary values are input at the bottom nodes, and then propagated upwards through the Boolean gates. The binary label is read off from the top node. This circuit is *deterministic* in that, for every \vee -gate, at most one of its inputs is 1 when the output is 1. It is *decomposable* in that, for every \wedge -gate, the inputs do not share features. The dDBC in the Figure is also *smooth*,

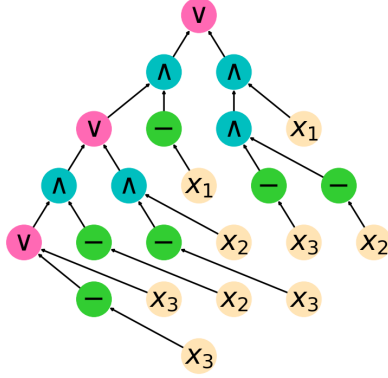


Figure 1: A dDBC.

in that sub-circuits that feed a same \vee -gate share the same features. It has a *fan-in* at most two, in that every \wedge -gate and \vee -gate have at most two inputs. We denote this subclass of dDBC with dDBCSFi(2).

In (Arenas et al. 2021b) it is established that *Shap* can be computed in polynomial time for dDBCSFi(2)-classifiers, assuming that the underlying probability distribution is the uniform, P^u , or the product distribution, P^\times . They are as follows for binary features: $P^u(e) := \frac{1}{2^N}$ and $P^\times(e) := \prod_{i=1}^N p_i(F_i(e))$, where $p_i(v)$ is the probability of value $v \in \{0, 1\}$ for feature F_i .

3 Compiling BNNs into dDBC

In order to compute *Shap* with a BNN, we convert the latter into a dDBC. *Shap* scores will be computed in the end with the resulting circuit and the polynomial time algorithm in (Arenas et al. 2021b). The transformation follows the following path, which we briefly describe next:

$$\text{BNN} \xrightarrow{(a)} \text{CNF} \xrightarrow{(b)} \text{SDD} \xrightarrow{(c)} \text{dDBC} \quad (3)$$

A BNN can be converted into a CNF formula (Shih, Darwiche, and Choi 2019; Narodytska et al. 2018), which, in its turn, can be converted into an SDD (Darwiche 2011b; Oztok and Darwiche 2014). It is also known that SDDs can be compiled into a formula in d-DNNF (deterministic and decomposable negated normal form) (Darwiche and Marquis 2002), which forms a subclass of dDBC. Actually, the resulting dDBC in (3) is eventually converted in polynomial time into a dDBCSFi(2).

Some of the steps in (3) may not be polynomial-time transformations, which we will discuss in more technical terms later in this section. However, we can claim at this stage that: (a) Any exponential cost of a transformation is kept under control by a usually small parameter. (b) The resulting dDBCSFi(2) is meant to be used multiple times, to explain different and multiple outcomes; and then, it may be worth taking a one-time, relatively high transformation cost. A good reason for our transformation path is the availability of implementations we can take advantage of.²

²The path in (3) is not the only way to obtain a dDBC. For

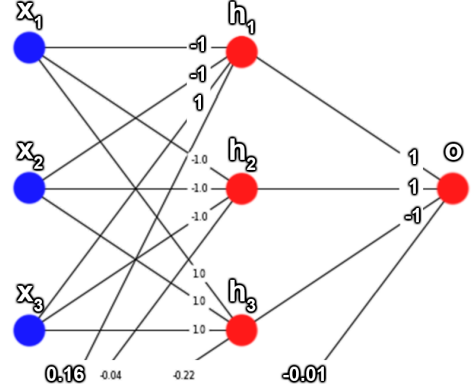


Figure 2: A BNN.

We will describe, explain and illustrate the conversion path (3) by means of a running example with a simple BNN, which is not the BNN used for our experiments. For them, we used a BNN with one hidden layer with 13 gates.

Example 1. The BNN in Figure 2 has hidden neuron gates h_1, h_2, h_3 , an output gate o , and three input gates, x_1, x_2, x_3 , that receive binary values. The latter represent, together, an input entity $\bar{x} = \langle x_1, x_2, x_3 \rangle$ that is being classified by means of a label returned by o . Each gate g is activated by means of a *step function* of the form:

$$\phi_g(\bar{i}) = sp(\bar{w}_g \bullet \bar{i} + b_g) := \begin{cases} 1 & \text{if } \bar{w}_g \bullet \bar{i} + b_g \geq 0, \\ -1 & \text{otherwise,} \end{cases} \quad (4)$$

which is parameterized by a vector of binary weights \bar{w}_g and a real-valued constant bias b_g .³ The \bullet is the inner vector product. For technical, non-essential reasons, for the gates, we use 1 and -1 instead of 0 and 1. However, we assume we have a single output gate, for which the activation function returns instead 1 or 0, for *true* or *false*, respectively.

For example, h_1 is *true*, i.e. outputs 1, for an input $\bar{x} = (x_1, x_2, x_3)$ iff $\bar{w}_{h_1} \bullet \bar{x} + b_{h_1} = (-1) \times x_1 + (-1) \times x_2 + 1 \times x_3 + 0.16 \geq 0$. Otherwise, h_1 is *false*, i.e. it returns -1 . Similarly, output gate o is *true*, i.e. returns label 1 for a binary input $\bar{h} = (h_1, h_2, h_3)$ iff $\bar{w}_o \bullet \bar{h} = 1 \times h_1 + 1 \times h_2 + (-1) \times h_3 - 0.01 \geq 0$, and 0 otherwise. \square

The first step, (a) in (3), consists in representing the BNN as a CNF formula, i.e. as a conjunction of disjunctions of *literals*, i.e. atomic formulas or their negations. For this, we adapt the approach in (Narodytska et al. 2018), in their case, to verify properties of BNNs. Contrary to them, we avoid the use of auxiliary variables since their posterior elimination conflicts with our need for determinism.

Each gate of the BNN is represented by a propositional formula, initially not necessarily in CNF, which, in its turn,

example, (Shi et al. 2020) describe a conversion of BNNs into OBDDs, which can also be used to obtain dDBC. However, the asymptotic time complexity is basically the same.

³It is also possible to use more complex activation functions, such as sigmoid and softmax functions, as long as the output is binarized.

is used as one of the inputs to gates next to the right. In this way, we eventually obtain a defining formula for the output gate. The formula is converted into CNF. The participating propositional variables are logically treated as *true* or *false*, even if they take numerical values 1 or -1 , resp.

Example 2. (example 1 cont.) Consider gate h_1 , with parameters $\bar{w} = \langle -1, -1, 1 \rangle$ and $b = 0.16$, and input $\bar{i} = \langle x_1, x_2, x_3 \rangle$. An input x_j is said to be *conveniently instantiated* if it has the same sign as w_j , and then, contributing to having a larger number on the LHS of the comparison in (4). E.g., this is the case of $x_1 = -1$. In order to represent as a propositional formula its output variable, also denoted with h_1 , we first compute the number, d , of conveniently instantiated inputs that are necessary and sufficient to make the LHS of the comparison in (4) greater than or equal to 0. This is the (only) case when h_1 becomes *true*; otherwise, it is *false*. This number can be computed in general by: (Narodytska et al. 2018)

$$d = \left\lceil (-b + \sum_{j=1}^{|\bar{i}|} w_j) / 2 \right\rceil + \# \text{ of negative weights in } \bar{w}. \quad (5)$$

In the case of h_1 , with 2 negative weights: $d = \lceil (-0.16 + (-1 - 1 + 1)) / 2 \rceil + 2 = 2$. With this, we can impose conditions on two input variables with the right sign at a time, considering all possible convenient pairs. For h_1 we obtain its condition to be true:

$$h_1 \longleftrightarrow (-x_1 \wedge -x_2) \vee (-x_1 \wedge x_3) \vee (-x_2 \wedge x_3). \quad (6)$$

This is DNF formula, directly obtained from considering all possible convenient pairs (which is already better than trying all cases of three variables at a time). However, there is a more expedite, iterative method that still uses the number of convenient inputs. In order to convey the bigger picture, we postpone the detailed description of this method (that is also used in our experiments) until Appendix A. Using this algorithm, we obtain an equivalent formula defining h_1 :

$$h_1 \longleftrightarrow (x_3 \wedge (-x_2 \vee -x_1)) \vee (-x_2 \wedge -x_1). \quad (7)$$

Similarly, we obtain defining formulas for gates h_2 and h_3 , and o : (for all of them, $d = 2$)

$$\begin{aligned} h_2 &\longleftrightarrow (-x_3 \wedge (-x_2 \vee -x_1)) \vee (-x_2 \wedge -x_1), \\ h_3 &\longleftrightarrow (x_3 \wedge (x_2 \vee x_1)) \vee (x_2 \wedge x_1), \\ o &\longleftrightarrow (-h_3 \wedge (h_2 \vee h_1)) \vee (h_2 \wedge h_1). \end{aligned} \quad (8)$$

Replacing the definitions of h_1, h_2, h_3 into (8), we finally obtain:

$$\begin{aligned} o &\longleftrightarrow (-[(x_3 \wedge (x_2 \vee x_1)) \vee (x_2 \wedge x_1)] \wedge \\ &\quad [(-x_3 \wedge (-x_2 \vee -x_1)) \vee (-x_2 \wedge -x_1)]) \vee \\ &\quad [(x_3 \wedge (x_2 \vee x_1)) \vee (x_2 \wedge x_1)] \wedge \\ &\quad [(-x_3 \wedge (-x_2 \vee -x_1)) \vee (-x_2 \wedge -x_1)] \wedge \\ &\quad [(x_3 \wedge (x_2 \vee x_1)) \vee (x_2 \wedge x_1)]. \end{aligned} \quad (9)$$

The final part of step (a) in path (3), requires transforming this formula into CNF. In this example, it can be taken

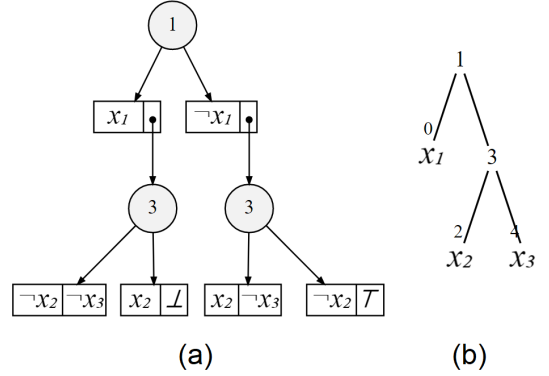


Figure 3: An SDD (a) and a vtree (b).

straightforwardly into CNF.⁴ The resulting CNF formula is, in its turn, simplified into a shorter and simpler new CNF formula by means of the *Confer* SAT solver (Manthey 2017). For this example, the simplified CNF formula is as follows:

$$o \longleftrightarrow (-x_1 \vee -x_2) \wedge (-x_1 \vee -x_3) \wedge (-x_2 \vee -x_3). \quad (10)$$

Having a CNF formula will be convenient for the next conversion steps along path (3). \square

Following with step (b) along path (3), the resulting CNF formula is transformed into a *Sentential Decision Diagram* (SDD) (Darwiche 2011b; Van den Broeck and Darwiche 2015), which, as a particular kind of *decision diagram* (Bollig and Butkus 2019), is a directed acyclic graph. So as the popular OBDDs (Bryant 1986), that SDDs generalize, they can be used to represent general Boolean formulas, in particular, propositional formulas (but without necessarily being *per se* propositional formulas).

Example 3. (example 2 cont.) Figure 3(a) shows an SDD, S , to be used for illustration. (C.f. (Bova 2016; Nakamura, Denzumi, and Nishino 2020) for precise definitions.) An SDD has different kinds of nodes. Those represented with encircled numbers are *decision nodes* (Van den Broeck and Darwiche 2015), e.g. ① and ③, that consider alternatives for the inputs (in essence, disjunctions). There are also nodes called *elements*. They are labeled with constructs of the form $[\ell_1 | \ell_2]$, where ℓ_1, ℓ_2 , called the *prime* and the *sub*, resp., are Boolean literals, e.g. x_1 and $\neg x_2$, including \top and \perp , for 1 or 0, resp. E.g. $[\neg x_2 | \top]$ is one of them. The *sub* can also be a pointer, \bullet , with an edge to a decision node. $[\ell_1 | \ell_2]$ represents two conditions that have to be satisfied simultaneously (in essence, a conjunction). An element without \bullet is a *terminal*.

An SDD represents (or defines) a total Boolean function $F_S : \langle x_1, x_2, x_3 \rangle \in \{0, 1\}^3 \mapsto \{0, 1\}$. For example, $F_S(0, 1, 1)$ is evaluated by following the graph downwards. Since $x_1 = 0$, we descent to the right; next via node ③ underneath, with $x_2 = 1$, we reach the instantiated leaf node labeled with $[1 | 0]$, a “conjunction”, with the second

⁴For our experiments, we programmed a simple algorithm that does this job, while making sure the generated CNF does not grow too much (c.f. Appendix A).

component due to $x_3 = 1$. We obtain $F_S(0, 1, 1) = 0$. \square

In SDDs, the orders of occurrence of variables in the diagram must be compliant with a so-called *vtree* (for “variable tree”).⁵ The connection between a vtree and an SDD refers to the compatibility between the partitions $[prime|sub]$ and the tree structure (c.f. Example 4 below). Depending on the chosen vtree, substructures of an SDD can be better reused when representing a Boolean function, e.g. a propositional formula, which becomes important to obtain a compact representation. An important feature of SDDs is that they can easily be combined via propositional operations, resulting in a new SDD (Darwiche 2011b).

A vtree for a set of variables \mathcal{V} is binary tree that is full, i.e. every node has 0 or 2 children, and ordered, i.e. the children of a node are totally ordered, and there is a bijection between the set of leaves and \mathcal{V} (Bova 2016).

Example 4. (example 3 cont.) Figure 3(b) shows a vtree, \mathcal{T} , for $\mathcal{V} = \{x_1, x_2, x_3\}$. Its leaves, 0, 2, 4, show their associated variables in \mathcal{V} . The SDD \mathcal{S} in Figure 3(a) is compatible with \mathcal{T} . Intuitively, the variables at \mathcal{S} ’s terminals, when they go upwards through decision nodes $\langle n \rangle$, also go upwards through the corresponding nodes n in \mathcal{T} . (C.f. (Bova 2016; Nakamura, Denzumi, and Nishino 2020; Bollig and Buttkus 2019) for a precise, recursive definition.)

The SDD \mathcal{S} can be straightforwardly represented as a propositional formula by interpreting decision points as disjunctions, and elements as conjunctions, obtaining $[x_1 \wedge ((-x_2 \wedge -x_3) \vee (x_2 \wedge \perp))] \vee [-x_1 \wedge ((x_2 \wedge -x_3) \vee (-x_2 \wedge \top))]$, which is logically equivalent to the formula on the RHS of (10) that represents the BNN. Accordingly, the BNN is represented by the SDD in Figure 3(a). \square

In our experiments and in the running example, we used the *PySDD* system (Meert and Choi 2018), which, given a CNF formula ψ , produces a vtree and a compliant SDD, both optimized in size, that represents the ψ (Choi and Darwiche 2013; Choi and Darwiche 2018).

This compilation takes space and time that are exponential only in the *tree-width*, $TW(\psi)$, of ψ , which is the tree-width of the graph \mathcal{G} associated to ψ (Darwiche 2011b; Oztok and Darwiche 2014). \mathcal{G} contains the variables as nodes, and undirected edges between any of them when they appear in a same clause. The tree-width measures how close the graph is to being a tree. The exponential upper-bound on the tree-width is a positive *fixed-parameter tractability* result (Flum and Grohe 2006) in that $TW(\psi)$ is in general much smaller $|\psi|$.

For example, the graph \mathcal{G} for the formula ψ on the RHS of (10) has x_1, x_2, x_3 as nodes, and edges between any pair of variables, which makes \mathcal{G} a complete graph. Since every complete graph has a tree-width equal to the number of nodes minus one, we have $TW(\psi) = 2$.

Our final transformation step consists in obtaining a dDBC from the resulting SDD, as follows: An SDD turns

⁵Extending OBDDs, which have special kinds of vtrees that capture the condition that variables in a path must always appear in the same order. This generalization makes SDDs much more succinct than OBDDs (Van den Broeck and Darwiche 2015; Bova 2016; Bollig and Buttkus 2019).

out to correspond to a d-DNNF Boolean circuit, for which decomposability and determinism hold, and has only variables as inputs to negation gates (Darwiche 2011b). The class d-DNNF is contained in dDBC.

The algorithm in (Arenas et al. 2021b) for Shap computing requires the dDBC a dDBCSFi(2). Every dDBC can be transformed in linear time into a dDBCSFi(2) (Arenas et al. 2021a). More details can be found in Appendix B.

Example 5. (example 3 cont.) By interpreting decision points and elements as disjunctions and conjunctions, resp., the SDD in Figure 3(a) can be easily converted into d-DNNF circuit. Notice that only variables are affected by negations. However, due to the children of node $\langle 3 \rangle$, that do not have the same variables, the directly resulting dBBC is not smooth (it has fan-in 2 though). It can be transformed into the dDBCSFi(2) in Figure 1. \square

4 Shap Computation: Experiments

The dataset “California Housing Prices” dataset was used for our experiments, in particular, to train a BNN and compute Shap scores. It can be downloaded from Kaggle (Nugent 2018) (it has been used before, e.g. in (Pace and Barry 1997)). It consists of 20,640 observations for 10 features with information on the block groups of houses in California, from the 1990 Census. Table 1 lists and describes the features, and the way in which they are binarized. The categorical feature #1 is one-hot encoded, giving rise to 5 binary features: #1_a, ..., #1_e. Accordingly, we end up with 13 binary input features, plus the binary output feature, #10. Accordingly, thirteen binary predictor features are used to predict a binary output, representing whether the median price at each block is high or low (i.e. above or below the average of the original #10).

We used the “Tensorflow” and “Larq” Python libraries to train a BNN with one hidden layer, with as many neurons as predictors, and one neuron for the output. For the hidden neurons, the activation functions are step function, as in (4), with outputs 1 or -1 , whereas the step function for the output returns 1 or 0. All weights were rounded to binary values (1 or -1) and the biases were kept as real numbers. The loss function employed was the *binary cross-entropy*, defined by $BCE(\bar{y}, \hat{y}) = -\frac{1}{|\bar{y}|} \sum_{i=1}^{|\bar{y}|} [y_i \log(\hat{y}_i) + (1 - y_i) \log(1 - \hat{y}_i)]$, where \hat{y} represents the labels predicted by the model and \bar{y} are the true labels. The BNN ended up having a binary cross-entropy of 0.9041, and an accuracy of 0.6580, based on the test dataset.

According to the transformation path (3), the constructed BNN was first represented as a CNF formula with 2,391 clauses. It has a tree-width of 12, which makes sense having a middle layer of 13 gates, each with all features as inputs. The CNF was transformed, via the SDD conversion, into a dDBCSFi(2), \mathcal{C} , which ended up having 18,671 nodes (without counting the negations affecting only input gates). Both transformations were programmed in Python. For the intermediate simplification of the CNF we used the SAT solver *Riss*. The initial transformation into CNF took 1.3 hrs. The conversion of the simplified CNF into the dDBCSFi(2) took 0.8276 secs.

Id #	Feature Name	Description	Original Values	Binarization
#1	<i>ocean_proximity</i>	A label of the location of the house w.r.t sea/ocean	Labels <i>1h_ocean</i> , <i>inland</i> , <i>island</i> , <i>near_bay</i> and <i>near_ocean</i>	Five features (one representing each label), for which 1 means a match with the value of <i>ocean_proximity</i> , and -1 otherwise
#2	<i>households</i>	The total number of households (a group of people residing within a home unit) for a block	Integer numbers from 1 to 6,082	1 (above average of the feature) or -1 (below average)
#3	<i>housing_median_age</i>	The median age of a house within a block (lower numbers means newer buildings)	Integer numbers from 1 to 52	1 (above average of the feature) or -1 (below average)
#4	<i>latitude</i>	The angular measure of how far north a block is (the higher value, the farther north)	Real numbers from 32.54 to 41.95	1 (above average of the feature) or -1 (below average)
#5	<i>longitude</i>	The angular measure of how far west a block is (the higher value, the farther west)	Real numbers from -124.35 to -114.31	1 (above average of the feature) or -1 (below average)
#6	<i>median_income</i>	The median income for households within a block (measured in tens of thousands of US dollars)	Real numbers from 0.50 to 15.00	1 (above average of the feature) or -1 (below average)
#7	<i>population</i>	The total number of people residing within a block	Integer numbers from 3 to 35,682	1 (above average of the feature) or -1 (below average)
#8	<i>total_bedrooms</i>	The total number of bedrooms within a block	Integer numbers from 1 to 6,445	1 (above average of the feature) or -1 (below average)
#9	<i>total_rooms</i>	The total number of rooms within a block	Integer numbers from 2 to 39,320	1 (above average of the feature) or -1 (below average)

Id #	Output	Description	Original Values	Labels
#10	<i>median_house_value</i>	The median house value for households within a block (measured in US dollars)	Integer numbers from 14,999 to 500,001	1 (above average of the feature) or 0 (below average)

Table 1: Features of the “California Housing Prices” dataset.

After the transformation, we had the possibility to compute **Shap** for a given input entity in three different ways:

- Directly on the BNN as a black-box model, i.e. using only its input/output relation for multiple calls, i.e. directly using formula (2);
- Similarly, using the circuit \mathcal{C} as a black-box model; and
- Using the efficient algorithm in (Arenas et al. 2021b), treating circuit \mathcal{C} as an open-box model. For completeness, it is reproduced here as Algorithm 1.

We performed these three computations for sets of 20, 40, 60, 80, and 100 input entities, to compare average times with increasing numbers of entities. In all cases, **Shap** was computed on the uniform probability distribution over the joint feature domain of size 2^{13} (using Algorithm 1 with the product distribution with $\frac{1}{2}$ for value 1). Everything was programmed in Python.

The experimental results we report below are the average **Shap** score for each feature over 100 entities; and the average time taken to compute them for 20, 40, 60, 80, 100 entities. For the cases (a) and (b) above, i.e. computations with black-box models, the classification labels were first computed for all entities in the population \mathcal{E} . After that, for each individual, fixed input entity e , when computing its **Shap** scores, all the other precomputed “counterfactual” versions

in \mathcal{E} were used in formula (2).⁶ The specialized algorithm for (c), the open-box case, does not require the precomputation of all entity labels. All experiments were run on *Google Colab* (with an NVIDIA Tesla T4 enabled).⁷

To report on **Shap** score computation, we used two different averages: over the original **Shap** scores, and over their absolute values. C.f. Figure 4. In this way, we can see the usual label each feature is associated with, and also its average relevance in absolute terms.

As expected, since the dDBC faithfully represent the BNN, we obtained exactly the same **Shap** scores under the three modes of computation, i.e. (a)-(c) above. Our results tell us that the three most relevant features for the classification label are $\#1_b$, $\#1_e$ and $\#6$.

The times taken to compute **Shap** in the three cases, (a)-(c), are shown in Figure 5, in logarithmic scale. For example, the time with the BNN for 100 entities was 7.7 hrs, whereas for the open-box dDBC it was 4.2 min. We observe a huge gain in performance with the use of the efficient al-

⁶The **Shap** scores reported in (Bertossi et al. 2020) were also computed in this way, but considering only the entity sample instead of the whole entity population.

⁷The complete code for *Google Colab* can be found at: <https://github.com/Jorvan758/dDBCSFi2>.

Algorithm 1: Shap Computation for dDBCSFi(2)

Input : A dDBCSFi(2) \mathcal{C} over feature set \mathcal{F} , fixed entity e and feature $F \in \mathcal{F}$, output gate g_{out} , and a rational probability $p(X = 1)$ for $X \in \mathcal{F}$. Below, $\mathcal{V}_g \subseteq \mathcal{F}$ contains the features that feed gate g .

Output: The $\text{Shap}(\mathcal{F}, \mathcal{G}_e, F)$ score for feature value of F in e (under the product distribution).

```

1 (Here every feature  $F \in \{0, 1\}$ , instead of  $F \in \{-1, 1\}$ )
2 for every gate  $g$  in  $\mathcal{C}$ , by bottom-up induction on  $\mathcal{C}$ 
3   if  $g$  is a constant gate with label  $a \in \{0, 1\}$  then
4      $\gamma_g^0 = a, \delta_g^0 = a$ 
5   else if  $g$  is a feature gate with  $\mathcal{V}_g = \{F\}$  then
6      $\gamma_g^0 = 1, \delta_g^0 = 0$ 
7   else if  $g$  is a feature gate with  $\mathcal{V}_g = \{X\}$  and  $X \neq F$ 
8     then
9        $\gamma_g^0, \delta_g^0 = p(X = 1), \gamma_g^1, \delta_g^1 = X(e)$ 
10    else if  $g$  is a  $\neg$ -gate with input gate  $g'$  then
11      for  $\ell \in \{0, \dots, |\mathcal{V}_g \setminus \{F\}|\}$ 
12         $\gamma_g^\ell = \binom{|\mathcal{V}_g \setminus \{F\}|}{\ell} - \gamma_{g'}^\ell, \delta_g^\ell = \binom{|\mathcal{V}_g \setminus \{F\}|}{\ell} - \delta_{g'}^\ell$ 
13    else if  $g$  is an  $\vee$ -gate with input gates  $g_1, g_2$  then
14      for  $\ell \in \{0, \dots, |\mathcal{V}_g \setminus \{F\}|\}$ 
15         $\gamma_g^\ell = \gamma_{g_1}^\ell + \gamma_{g_2}^\ell, \delta_g^\ell = \delta_{g_1}^\ell + \delta_{g_2}^\ell$ 
16    else if  $g$  is an  $\wedge$ -gate with input gates  $g_1, g_2$  then
17      for  $\ell \in \{0, \dots, |\mathcal{V}_g \setminus \{F\}|\}$ 
18         $\gamma_g^\ell = \sum_{\substack{\ell_1 \in \{0, \dots, |\mathcal{V}_{g_1} \setminus \{F\}|\} \\ \ell_2 \in \{0, \dots, |\mathcal{V}_{g_2} \setminus \{F\}|\} \\ \ell_1 + \ell_2 = \ell}} \gamma_{g_1}^{\ell_1} \cdot \gamma_{g_2}^{\ell_2}$ 
19         $\delta_g^\ell = \sum_{\substack{\ell_1 \in \{0, \dots, |\mathcal{V}_{g_1} \setminus \{F\}|\} \\ \ell_2 \in \{0, \dots, |\mathcal{V}_{g_2} \setminus \{F\}|\} \\ \ell_1 + \ell_2 = \ell}} \delta_{g_1}^{\ell_1} \cdot \delta_{g_2}^{\ell_2}$ 
20   $\text{Shap}(\mathcal{F}, \mathcal{G}_e, F) =$ 
21     $\sum_{k=0}^{|\mathcal{F}|-1} \frac{k! (|\mathcal{F}|-k-1)!}{|\mathcal{F}|!} \cdot [(F(e) - p(F = 1)) \cdot (\gamma_{g_{out}}^k - \delta_{g_{out}}^k)]$ 

```

gorithm on the open-box dDBC. Those times do not show the one-time computation for the transformation of the BNN into the dDBC.

The difference in time between the BNN and the black-box dDBC, i.e. cases (a) and (b), resides in the fact that the BNN allows some batch processing for the initial label predictions, which translates into just 6 matrix operations (2 weight multiplications, 2 bias additions, and 2 activations), whereas with the dDBC the classifications are made one at a time.

5 Conclusions

The main objective of the research we reported about has been twofold. On one side, we have showed the convenience of applying knowledge compilation techniques to obtain explanations for ML-based models. On the other side, we have also established the huge difference in performance when computing explanation scores for a classifier when treating it as a black-box vs. treating it as an open-box.

In relation to the knowledge compilation phase, we emphasize once more, that the effort invested in transforming the BNN into a dDBC is something we incur once, being the compilation of the BNN into a CNF the most expensive step. In comparison, the subsequent transformations into SDD,

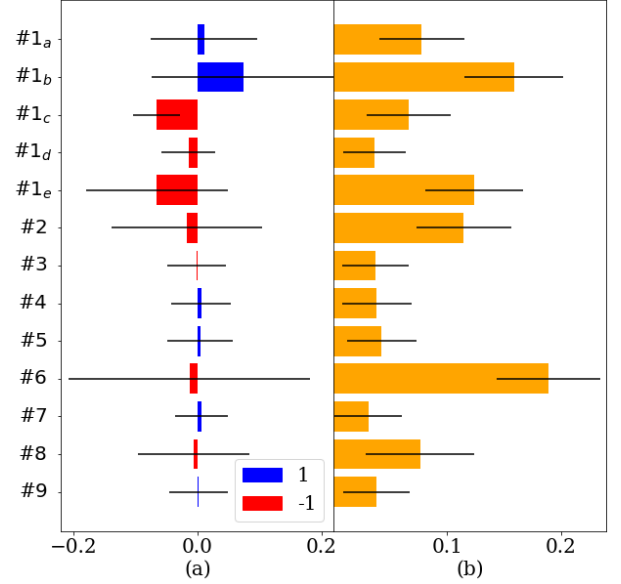


Figure 4: Average Shap score for each feature with 100 entities (a) (where red means an average closer to -1 and blue closer 1), and for their absolute values (b).

and the required dDBC take a very small time.

Despite the intrinsic complexity involved, there is much room for improving the algorithmic and implementation aspects of the BNN compilation. The same applies to the implementation of the efficient Shap computation algorithm.

The resulting circuit can be used to obtain Shap scores multiple times, and for multiple inputs. We have showed that the performance gain in Shap computation with the circuit exceeds by far both the compilation time and the Shap computation time for the BNN used a black-box classifier. Furthermore, the resulting circuit can be used for other purposes, such as *verification* of general properties of the classifier (Narodytska et al. 2018; Darwiche and Hirth 2020).

When we can easily obtain explanation scores, such as Shap, we have an additional tool to analyze the goodness of our classifier. Obtaining unexpected or surprising explanations may invite us to reconsider the whole machine learning process, starting from the original dataset on, all the way to the deployment of the classifier.

We computed Shap scores using the uniform distribution on the entity population. There are a few issues to discuss in this regard. First, it is computationally costly to use it with a large number of features. One could use instead the *empirical distribution* associated to the dataset, as in (Bertossi et al. 2020) for black-box Shap computation. This would require appropriately modifying the applied algorithm, which is left for future work. Secondly, and more generally, the uniform distribution does not capture possible dependencies among features. The algorithm is still efficient with the *product distribution*, which also suffers from imposing feature independence (c.f. (Bertossi et al. 2020) for a discussion of its empirical version and related issues). It would be interesting to explore to what extent other distributions could be used in

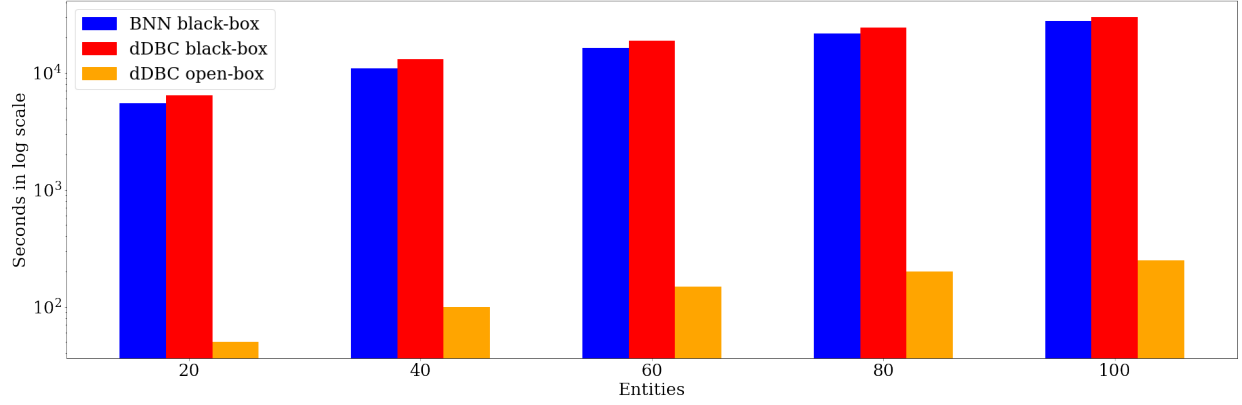


Figure 5: Seconds taken to compute Shap on 20, 40, 60, 80 and 100 entities; using the BNN as a black-box (blue bar), the dDBC as a black-box (red bar), and the dDBC as an open-box (orange bar). Note that the vertical axis employs a logarithmic scale.

combination with our efficient algorithm.

Independently from the algorithmic and implementation aspects of *Shap* computation, an important research problem has to do with bringing *domain knowledge* or *domain semantics* into the definitions and computations of attribution scores, to obtain more meaningful and interpretable results. This additional knowledge could come, for example, in declarative terms, expressed as *logical constraints*. They could be used to appropriately modify the algorithm or the underlying distribution (Bertossi 2021). It is likely that domain knowledge can be more easily brought into a score computation when it is done on a logic-based classifier, such as a dDBC.

In this work we have considered only binary NNs. It would be interesting to investigate to what extent our methods can be applied to non-binary NNs. There is work on binarized NNs (Qin et al. 2020; Yuan and Agaian 2021; Simons and Lee 2019), but it is not clear whether that would be a feasible way to go.

Acknowledgments

Our special thanks go to: (a) Arthur Choi, for the use of the PySDD repository, and his kind and permanent advice on how to use it. And also answering more fundamental questions; (b) Andy Shih, for sharing some preliminary code for the conversion of BNNs into CNF, and explaining many issues; (c) Norbert Manthey, for his Riss tool collection repository, answering questions about its use and the simplification of CNF formulas; (d) Maximilian Schleich, for sharing some preliminary code for the black-box computation of *Shap*; and (e) Adnan Darwiche, for sharing useful insights.

Part of this work was funded by ANID - Millennium Science Initiative Program - Code ICN17002; and “Centro Nacional de Inteligencia Artificial” CENIA, FB210017 (Financiamiento Basal para Centros Científicos y Tecnológicos de Excelencia de ANID), Chile. Both CENIA and SKEMA Canada funded Jorge León’s visit to Montreal. L. Bertossi is a Professor Emeritus at Carleton University, Ottawa, Canada; and a Senior Fellow of the Universidad Adolfo Ibáñez (UAI), Chile.

A BNN to CNF Formula

Our conversion of the BNN into a CNF formula is inspired by a technique introduced in (Narodytska et al. 2018). However, it cannot be applied straightforwardly since it introduces auxiliary variables, whose final elimination becomes a challenge for our purposes. The application of a *variable forgetting* technique (Oztok and Darwiche 2017) turns out to damage the required determinism of the dDBC. Accordingly, it is necessary to adapt the conversion technique, avoiding the use of the auxiliary variables. We sketch the approach in the following. C.f. Example 2 for intuitions and motivation.

Consider a BNN receiving ℓ_0 input features, say $\bar{x} = \langle x_1, \dots, x_{\ell_0} \rangle$. The BNN has m hidden layers, each layer z (from 1 to m) with ℓ_z neurons. A neuron in layer z receives the input vector $\bar{i} = \langle i_1, \dots, i_{\ell_{z-1}} \rangle$. The output layer has a single neuron. As in Section 3, all weights and features are -1 or 1 , with the activation functions returning -1 or 1 , except for the output layer that returns 0 or 1 .

To convert the BNN into a CNF formula, we do it layer-wise from input to output. All the neurons in a layer can be converted in parallel. For every neuron gate g , we encode the case when it returns 1 , representing its activation function $sp(\bar{w}_g \bullet \bar{i} + b_g)$ as a CNF formula. For this, we compute, as in (5), the number d_g of inputs to be instantiated for the output to be 1 .

For each neuron g on the first layer, and to conveniently manage the whole process, we construct a matrix-like structure M_g of dimension $|\bar{i}| \times d_g$, whose components $c_{k,t}$ are propositional formulas.

$$M_g = \begin{bmatrix} w_1 \cdot i_1 & false & false & \dots & false \\ w_2 \cdot i_2 & w_2 \cdot i_2 & false & \dots & false \\ \vee c_{1,1} & \wedge c_{1,1} & & & \\ w_3 \cdot i_3 & (w_3 \cdot i_3) & w_3 \cdot i_3 & \dots & false \\ \vee c_{2,1} & \wedge c_{2,1} & \wedge c_{2,2} & & \\ & \vee c_{2,2} & & & \\ \dots & \dots & \dots & \dots & \dots \\ w_{|\bar{i}|} \cdot i_{|\bar{i}|} \vee & (w_{|\bar{i}|} \cdot i_{|\bar{i}|} \vee & (w_{|\bar{i}|} \cdot i_{|\bar{i}|} \vee & \dots & (w_{|\bar{i}|} \cdot i_{|\bar{i}|} \wedge \\ c_{|\bar{i}|-1,1} & \wedge c_{|\bar{i}|-1,1}) & \wedge c_{|\bar{i}|-1,2}) & & c_{|\bar{i}|-1,d_g-1}) \\ & \vee c_{|\bar{i}|-1,2} & \vee c_{|\bar{i}|-1,3} & & \vee c_{|\bar{i}|-1,d_g} \end{bmatrix}$$

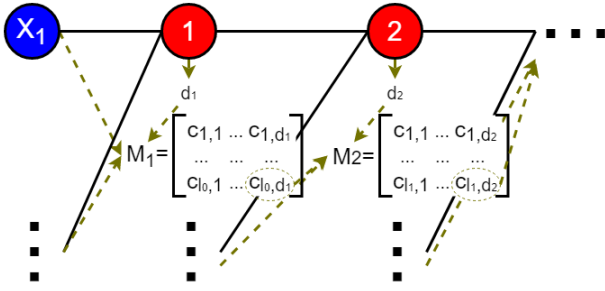


Figure 6: From BNN to CNF (fragment). Initial variables (in blue) are inputs for first layer. Neurons ① and ② (in red) have d_1, d_2 and arrays M_1, M_2 , whose bottom, right entries encode ① and ②, resp. They are given as inputs to the arrays for the next layer.

In this array, a term of the form $w_k \cdot i_k$ does not represent a number, but a propositional formula, namely i_k if $w_k = 1$, and $\neg i_k$ if $w_k = -1$. Every M_g is filled in a row-wise manner starting from the top, and then column-wise from left to right. The formula that will be passed over to the next layer to the right is the last entry, $c_{|i| \times d_g}$ (highlighted).

Only in the arrays for the first layer we find new propositional variables, for the inputs. For the next layers, the whole output formulas from the previous layer are passed over as inputs, and they become the i_k 's just mentioned. In this way, no auxiliary variables other than those for the initial inputs are created. Each row represents the number of the first $k \in \{1, \dots, |i|\}$ inputs considered for the encoding, and each column, the threshold $t \in \{1, \dots, d_g\}$ to surpass (meaning that at least t inputs should be instantiated conveniently). For every component where $k < t$, the threshold cannot be reached, which makes every component in the upper, right triangle to be *false*.

For explanation, the first row of M_g has the first entry $w_1 \cdot i_1$, and *false* for the rest. Each entry $c_{k,1}$ of the first column becomes $w_k \cdot i_k \vee c_{k-1,1}$. For any other component $c_{k,t}$, $t > 1$, we use $(w_k \cdot i_k \wedge c_{k-1,t-1}) \vee c_{k-1,t}$. So, the lower right component $c_{|i|,d_g}$ of M_g ends up being the encoding of neuron g , and it is the only formula that will be used in the encodings for the next layer. All the M_g 's for a layer can be generated in parallel, as their encodings do not influence each other.

For the second layer, we take as inputs the encodings c_{ℓ_0, d_g} from the previous one, and we keep repeating this conversion. In other words, we compute d_g and M_g for every neuron g in the new layer, taking the previous encodings as inputs. The resulting c_{ℓ_1, d_g} s are given as inputs for the next layer, and we iterate all the way until the last layer. For illustration, c.f. Figure 6.

From the array M_o for the single output neuron, o , at the last layer, we extract the component c_{ℓ_m, d_o} , which becomes the propositional encoding of the whole BNN. This is a propositional formula that is next converted into a CNF formula, which in its turn is further simplified (c.f. Section 3).⁸

Departing from (Narodytska et al. 2018), we use the arrays M_g , which help us obtain a final propositional formula

⁸Actually, every entry in an array M_g is immediately transformed into CNF and simplified, avoiding the iterative creation of extremely long, complex and non-CNF formulas.

Algorithm 2: From dDBC to dDBCSFi(2)

Input : Original *dDBC* (starting from root node).
Output: A *dDBCSFi(2)* equivalent to the given *dDBC*.

```

1 function FIX_NODE(dDBC_node)
2   if dDBC_node is a disjunction then
3      $c_{new} = false$ 
4     for each subcircuit sc in dDBC_node
5        $sc_{fixed} = FIX\_NODE(sc)$ 
6       if  $sc_{fixed}$  is a true value or is equal to  $\neg c_{new}$ 
7         then
8           return true
9     else if  $sc_{fixed}$  is not a false value then
10      for each variable v in  $c_{new}$  and not in
11         $sc_{fixed}$ 
12        |  $sc_{fixed} = sc_{fixed} \wedge (v \vee \neg v)$ 
13      for each variable v in  $sc_{fixed}$  and not in
14         $c_{new}$ 
15        |  $c_{new} = c_{new} \wedge (v \vee \neg v)$ 
16       $c_{new} = c_{new} \vee sc_{fixed}$ 
17     return  $c_{new}$ 
18   else if dDBC_node is a conjunction then
19      $c_{new} = true$ 
20     for each subcircuit sc in dDBC_node
21        $sc_{fixed} = FIX\_NODE(sc)$ 
22       if  $sc_{fixed}$  is a false value or is equal to  $\neg c_{new}$ 
23         then
24           return false
25       else if  $sc_{fixed}$  is not a true value then
26          $c_{new} = c_{new} \wedge sc_{fixed}$ 
27     return  $c_{new}$ 
28   else if dDBC_node is a negation then
29     return  $\neg FIX\_NODE(\neg dDBC\_node)$ 
30   else
31     return dDBC_node
32 dDBCSFi(2) = FIX_NODE(root_node)

```

that can be more easily transformed into a deterministic BC. On the negative side, our approach is computationally more costly, but again, a cost in which we incur once.

B dDBC to dDBCSFi(2)

It is possible to transform an arbitrary dDBC into an dDBCSFi(2), as follows. In a bottom-up fashion, as suggested in (Arenas et al. 2021a), fan-in 2 is achieved by simply rewriting every \wedge -gate (resp., and \vee -gate) of fan-in $m > 2$ with a chain of $m - 1$ \wedge -gates (resp., \vee -gates) of fan-in 2.

After that, to enforce smoothness, for every disjunction gate (now with a fan-in 2) of subcircuits C_1 and C_2 , find the set of all variables present in C_1 and not in C_2 (denoted V_{1-2}), along with all the ones in C_2 and not in C_1 (denoted V_{2-1}). For every variable $v \in V_{2-1}$, redefine C_1 as $C_1 \wedge (v \vee \neg v)$. Similarly, for every variable $v \in V_{1-2}$, redefine C_2 as $C_2 \wedge (v \vee \neg v)$. For example, for $(x_1 \wedge x_2 \wedge x_3) \vee (x_2 \wedge \neg x_3)$, becomes $((x_1 \wedge x_2) \wedge x_3) \vee ((x_2 \wedge \neg x_3) \wedge (x_1 \vee \neg x_1))$.

The algorithm for the conversion of dDBC into dDBCSFi(2) that we implemented can be found as Algorithm 2. Since this transformation requires going through each node once, the time complexity is linear in the number of nodes of the dDBC.

References

- Arenas, M.; Barceló, P.; Bertossi, L.; and Monet, M. 2021a. On the Complexity of SHAP-Score-Based Explanations: Tractability via Knowledge Compilation and Non-Approximability Results. *ArXiv* 2104.08015. Extended version of (Arenas et al. 2021b).
- Arenas, M.; Barceló, P.; Bertossi, L.; and Monet, M. 2021b. The Tractability of SHAP-Score-Based Explanations for Classification over Deterministic and Decomposable Boolean Circuits. In *Proceedings of the 35th AAAI Conference on Artificial Intelligence*, 6670–6678.
- Bertossi, L.; Li, J.; Schleich, M.; Suciu, D.; and Vagena, Z. 2020. Causality-Based Explanation of Classification Outcomes. In *Proceedings of the 4th International Workshop on "Data Management for End-to-End Machine Learning" (DEEM) at ACM SIGMOD/PODS*, 1–10. Posted as Corr ArXiv Paper 2003.06868.
- Bertossi, L. 2021. Declarative Approaches to Counterfactual Explanations for Classification. *Theory and Practice of Logic Programming* 1–35. <https://doi.org/10.1017/S1471068421000582>. Posted as Corr ArXiv Paper 2011.07423.
- Bertossi, L. 2022. Score-Based Explanations in Data Management and Machine Learning: An Answer-Set Programming Approach to Counterfactual Analysis. In Simkus, M., and Varzinczak, I., eds., *Reasoning Web. Declarative Artificial Intelligence, Lecture Notes in Computer Science 13100*, 145–184. Springer.
- Bollig, B., and Buttkus, M. 2019. On the Relative Succinctness of Sentential Decision Diagrams. *Theory of Computing Systems* 63(6):1250–1277.
- Bova, S. 2016. SDDs Are Exponentially More Succinct than OBDDs. In *Proceedings of the 30th AAAI Conference on Artificial Intelligence*, 929–935.
- Bryant, R. E. 1986. Graph-Based Algorithms for Boolean Function Manipulation. *IEEE Transactions on Computers* C-35(8):677–691.
- Chockler, H., and Halpern, J. 2004. Responsibility and Blame: A Structural-Model Approach. *Journal of Artificial Intelligence Research* 22:93–115.
- Choi, A., and Darwiche, A. 2013. Dynamic Minimization of Sentential Decision Diagrams. In *Proceedings of the 27th AAAI Conference on Artificial Intelligence*, 187–194.
- Choi, A., and Darwiche, A. 2018. *SDD Advanced-User Manual Version 2.0*. Automated Reasoning Group, UCLA.
- Darwiche, A., and Hirth, A. 2020. On The Reasons Behind Decisions. In *Proceedings of the 24th European Conference on Artificial Intelligence*, 712–720.
- Darwiche, A., and Marquis, P. 2002. A Knowledge Compilation Map. *Journal of Artificial Intelligence Research* 17(1):229–264.
- Darwiche, A. 2011a. On the Tractable Counting of Theory Models and its Application to Truth Maintenance and Belief Revision. *Journal of Applied Non-Classical Logics* 11(1-2):11–34.
- Darwiche, A. 2011b. SDD: A New Canonical Representation of Propositional Knowledge Bases. In *Proceedings of the 22th International Joint Conference on Artificial Intelligence (IJCAI-11)*, 819–826.
- Flum, J., and Grohe, M. 2006. *Parameterized Complexity Theory*. Springer.
- Guidotti, R.; Monreale, A.; Ruggieri, S.; Turini, F.; Giannotti, F.; and Pedreschi, D. 2018. A Survey of Methods for Explaining Black Box Models. *ACM Computing Surveys* 51(5):1–42.
- Halpern, J. Y., and Pearl, J. 2005. Causes and Explanations: A Structural-Model Approach. Part I: Causes. *The British Journal for the Philosophy of Science* 56(4):843–887.
- Lundberg, S. M., and Lee, S.-I. 2017. A Unified Approach to Interpreting Model Predictions. In *Proceedings of the 31st International Conference on Neural Information Processing Systems*, 4768–4777. ArXiv Paper 1705.07874.
- Lundberg, S.; Erion, G.; Chen, H.; DeGrave, A.; Prutkin, J.; Nair, B.; Katz, R.; Himmelfarb, J.; Bansal, N.; and Lee, S.-I. 2020. From Local Explanations to Global Understanding with Explainable AI for Trees. *Nature Machine Intelligence* 2(1):56–67. ArXiv Paper 1905.04610.
- Manthey, N. 2017. Riss tool collection. <https://github.com/nmanthey/riss-solver>.
- Meert, W., and Choi, A. 2018. Python Wrapper Package to Interactively use Sentential Decision Diagrams (SDD). <https://github.com/wannesm/PySDD>.
- Nakamura, K.; Denzumi, S.; and Nishino, M. 2020. Variable Shift SDD: A More Succinct Sentential Decision Diagram. In *Proceedings of the 18th International Symposium on Experimental Algorithms (SEA 2020), Leibniz International Proceedings in Informatics 160*, 22:1–22:13.
- Narodytska, N.; Kasiviswanathan, S.; Ryzhyk, L.; Sagiv, M.; and Walsh, T. 2018. Verifying Properties of Binarized Deep Neural Networks. In *Proceedings of the 32nd AAAI Conference on Artificial Intelligence*, 6615–6624.
- Nugent, C. 2018. California Housing Prices. <https://www.kaggle.com/datasets/camnugent/california-housing-prices>.
- Oztok, U., and Darwiche, A. 2014. On Compiling CNF into Decision-DNNF. In *Proceedings of the 20th International Conference on Principles and Practice of Constraint Programming, Lecture Notes in Computer Science 8656*, 42–57.
- Oztok, U., and Darwiche, A. 2017. On Compiling DNNFs without Determinism. *ArXiv* 1709.07092.
- Pace, R. K., and Barry, R. 1997. Sparse Spatial Autoregressions. *Statistics & Probability Letters* 33(3):291–297.
- Qin, H.; Gong, R.; Liu, X.; Bai, X.; Song, J.; and Sebe, N. 2020. Binary Neural Networks: A Survey. *Pattern Recognition* 105:107281.
- Ras, G.; Xie, N.; van Gerven, M.; and Doran, D. 2022. Explainable Deep Learning: A Field Guide for the Uninitiated. *Journal of Artificial Intelligence Research* 73:329–396.
- Roth, A. E. e. 1988. *The Shapley Value: Essays in Honor of Lloyd S. Shapley*. Cambridge University Press.

- Rudin, C. 2019. Stop Explaining Black Box Machine Learning Models for High Stakes Decisions and Use Interpretable Models Instead. *Nature Machine Intelligence* 1:206–215. ArXiv Paper 1811.10154.
- Shapley, L. S. 1953. A Value for n-Person Games. In *Contributions to the Theory of Games (AM-28)*, volume 2, 307–318.
- Shi, W.; Shih, A.; Darwiche, A.; and Choi, A. 2020. On Tractable Representations of Binary Neural Networks. In *Proceedings of the 17th International Conference on Principles of Knowledge Representation and Reasoning*, 882–892. ArXiv Paper 2004.02082.
- Shih, A.; Darwiche, A.; and Choi, A. 2019. Verifying Binarized Neural Networks by Angluin-Style Learning. In *Proceedings of the Theory and Applications of Satisfiability Testing - SAT 2019, Lecture Notes in Computer Science 11628*, 354–370.
- Simons, T., and Lee, D.-J. 2019. A Review of Binarized Neural Networks. *Electronics* 8(6):661.
- Van den Broeck, G., and Darwiche, A. 2015. On the Role of Canonicity in Knowledge Compilation. In *Proceedings of the 29th AAAI Conference on Artificial Intelligence*, 1641–1648.
- Van den Broeck, G.; Lykov, A.; Schleich, M.; and Suciu, D. 2021. On the Tractability of SHAP Explanations. In *Proceedings of the 35th AAAI Conference on Artificial Intelligence*, 6505–6513.
- Yuan, C., and Agaian, S. S. 2021. A Comprehensive Review of Binary Neural Network. *ArXiv* 2110.06804.